Canadian Conference - Pacific Conference on Earthquake Engineering 2023

Vancouver, British Columbia

June 25th – June 30th, 2023

Design Considerations of Braced Frame Bolted Glulam Timber Connections with Internal Steel Plates

Zoe Baird[1], Joshua Woods[2*], Christian Viau[3] and Ghasan Doudak[4]

[1]Graduate Student, Department of Civil Engineering, Queen's University, Kingston, ON, Canada
[2]Assistant Professor, Department of Civil Engineering, Queen's University, Kingston, ON, Canada
[3]Assistant Professor, Department of Civil & Environmental Engineering, Carleton University, Ottawa, ON, Canada
[4]Professor, Department of Civil Engineering, University of Ottawa, Ottawa, ON, Canada
[*]joshua.woods@queensu.ca (Corresponding Author)

ABSTRACT

While the demand for mass timber structures in Canada increases, significant questions remain surrounding the design and detailing requirements for timber braced frames under earthquake loads. Timber braced frame buildings typically rely on the connections, which consist of steel plates and dowel-type fasteners. Under earthquake loads, the steel dowels are intended to yield and dissipate energy. Such connections need to have sufficient ductility to achieve the system-level ductility required in the design of timber braced frames (e.g. limited or moderate ductility). However, the current Engineering Design in Wood standard (CSA O86) lacks guidance on how to detail bolted brace connections to achieve the system-level ductility in the National Building Code of Canada [1-2]. The objective of this research is to investigate the behaviour of bolted connections with slotted-in steel plates under cyclic loading and establish detailing requirements to ensure ductile connection behaviour. To accomplish this objective, a prototype 8-storey timber braced frame building was designed. The goal of the design was to achieve ductile connections that ultimately could lead to moderately ductile system-level behaviour. The ductility at the component-level was validated through full-scale experimental connection tests under monotonic and cyclic loading. The connection-level ductility, behaviour mechanisms, and energy dissipation capacity of the connection were evaluated.

Keywords: mass timber, brace connections, ductility, cyclic loading, experimental testing

INTRODUCTION

Despite the increased popularity of mass timber construction in Canada, there are still knowledge gaps surrounding their performance under lateral loads, including wind and earthquake loads. Examples of seismic force-resisting systems (SFRS) which have been used and studied in Canada include cross-laminated timber (CLT) shear wall systems and timber braced frames [3-4]. Braced frames are effectively vertical cantilevered trusses in which the columns and beams that form the truss carry the gravity loads and the braces resist lateral wind and earthquake loads. In practice, braced frames can form stiff and efficient lateral load resisting systems. In contrast to a conventional steel braced frame, which dissipates energy through yielding of the steel braces in tension, timber braced frames achieve their ductility and dissipate energy through yielding of the brace connections.

The National Building Code of Canada (NBCC) recognizes both limited and moderately ductile timber braced frames as lateral-load resisting systems [2]. Limited ductility braced frames have a ductility related modification factor (R_d) of 1.5 and an overstrength factor (R_o) of 1.5. The ductility related and overstrength factors for moderately ductile braced frames are 2.0 and 1.5, respectively. The ductility related modification factor (R_d) for moderate or limited ductility systems influences the magnitude of the base shear used to design the components of a structure, including those that are capacity protected and the fuses, which for a brace timber frame are the end connections. Thus, there is an incentive to specify a higher level of ductility resulting in lower design loads.

To achieve moderate or limited ductility it is common to use slotted-in steel plates and slender steel dowel-type fasters (e.g. bolts or tight-fit pins) in the brace end connections, which are intended to yield before the onset of brittle failure modes, resulting in the ability to sustain large plastic deformations and stable hysteretic performance under cyclic loading [5]. However, littleto-no guidance exists in the Engineering Design in Wood Standard (CSA O86) on how to detail these types of brace connections (e.g., dowel slenderness, spacing) to achieve the system-level ductility that is specified in the NBCC [1-2].

This study aims to develop an improved understanding of the behaviour of glued-laminated (glulam) timber brace connections with steel bolts and slotted-in steel plates under cyclic loading. The specific objectives of the study are to: (1) design a prototype 8-storey braced frame for a Canadian region of moderate seismicity, (2) evaluate the seismic behaviour of a representative connection from the braced frame, including the connection stiffness, strength, and ductility (3) examine the influence of connection design parameters, including bolt spacing and dowel slenderness, on connection ductility, and (4) compare connection strength and failure mode with those from the Engineering Design in Wood standard (CSA O86-19).

PROTOTYPE BUILDING DESIGN

Building Geometry

An 8-storey prototype mass timber braced frame building was designed for a site in Ottawa, Ontario. This location represents a region of moderate seismicity in Central Canada where the use of limited or moderately ductile braced frames would be advantageous. The structure was designed in accordance with the NBCC [2] and CSA O86-19 [1]. Figure 1 shows the plan view of the structure and the elevation view of a representative braced timber frame. The building is square and has seven bays in each direction, totalling 1764 m^2 in floor area. The height of each storey is 3.7 m and the width of each bay is 6 m. Two of the seven bays on each exterior wall are braced frames in a chevron configuration, which is the primary lateral load-resisting structural system. The beams, columns, and braces in the prototype structure were fabricated of spruce-pine glulam and the floor slab consisted of one-way cross-laminated timber panels, the properties of which were determined according to CSA O86-19 [1].

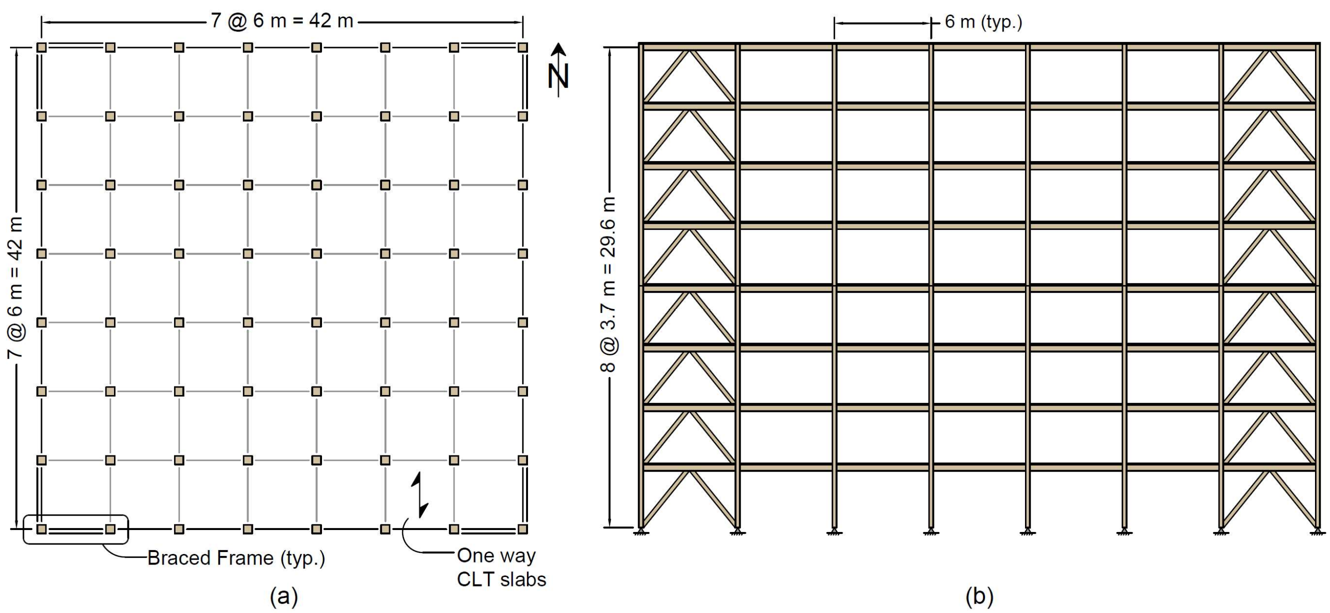

Figure 1. Prototype Building layout: (a) plan view and (b) braced frame elevation (N-S).

Design of Gravity Load Resisting System

All five load cases from the NBCC were used to determine the design loads and a 3-dimensional (3D) model of the structure in S-FRAME was used to determine the design forces, moments, and displacements experienced by the structural framing members under gravity loads [1]. Table 1 shows a summary of the gravity loads used in the design of the prototype structure. The occupancy of the structure was assumed to be office type and the dead load included an allowance for mechanical and electrical, flooring materials, partitions, fireproofing, and wood framing.

Table 1. Summary of Gravity Loads.

	Roof Load (kPa)	**Floor Load (kPa)**
Dead Load	1.88	2.64
Live Load	1.00	2.40
Snow Load	2.32	-

CLT floor slabs are assumed for self-weight calculations. It was determined that 5-ply CLT slabs with a ply thickness of 35 mm are required based on the Panel Selection Tables in the Wood Design Manual and the Nordic X-Lam Technical Guide [7]. Table 2 shows a summary of the member sizes for the gravity load resisting system.

Table 2. Gravity Member Size Summary (units in mm).

	Storeys 1-2	**Storeys 3-4**	**Storeys 5-6**	**Storeys 7-8**
Interior Beam	265 x 456	265 x 456	265 x 456	265 x 456
Exterior Beam	175 x 380	175 x 380	175 x 380	175 x 380
Interior Column	365 x 456	315 x 380	265 x 304	265 x 304
Exterior Column	315 x 342	265 x 266	215 x 228	215 x 228
CLT Slab	143-5s	143-5s	143-5s	143-5s

Design of Lateral Load Resisting System

Earthquake loads for the prototype building were calculated in accordance with the equivalent static force procedure (ESFP) from the NBCC and were used to design the braced frames. The base shear (V) was calculated using the design spectrum for Ottawa City Hall (45.4° N, 75.7° W), which is shown in Figure 2. The building was assumed to be on a site designated as class C and the seismic weight was determined for each floor using 100% of the dead loads and 25% of the snow load on the roof.

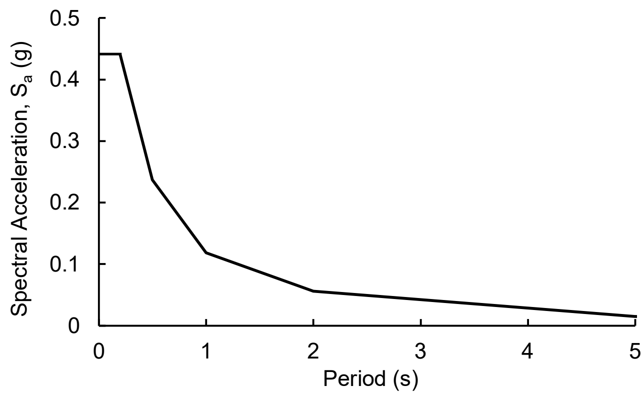

Figure 2. Design spectrum for Ottawa (City Hall).

The fundamental period of the building (T_a) was estimated using $T_a = 0.1N$ where N is the number of storeys in the building, which resulted in a fundamental period of 0.8 s for the 8-storey structure. The NBCC states that for braced frames T_a can be taken as up to $2T_a$ if justified through established methods of mechanics or a structural model, which was the case for the prototype structure in this study [2].

Seismic design using the NBCC uses a life-safety design objective and assumes that the structure will experience some damage under a design-level earthquake, and thus, permits a structure to be designed for lower seismic loads depending on its ductility. A ductility-related force modification factor (R_d) was first introduced in the 2005 publication of the NBCC and reduces the base shear (V) based on the system ductility and accounts for the capacity of a building to deform inelastically under earthquake (cyclic) loading without losing a significant amount of strength. Since the 2005 publication, values of R_d have been established for a wider range of structural systems, including moderate and limited ductility braced frames, for which it specifies R_d values of 2.0 and 1.5, respectively. The minimum lateral earthquake design force (V) at the base of the structure was calculated using Eq. (1):

$$V = \frac{S(T_a) M_v I_E W}{R_d R_o} \tag{1}$$

where S_a is the 5% damped spectral response acceleration at the building fundamental period T_a, M_v is the higher mode factor, I_E is the earthquake importance factor, which is 1.0 for normal importance structures, W is the total seismic weight of the building (1.0*D*+0.25*S*), and R_o is an overstrength factor that accounts for the dependable portion of reserve strength in a structure. For the design of the prototype building in this paper, the site coefficients were 1.0 for site class C conditions, the structure was assumed to be of normal importance (I_E = 1.0), the total seismic weight was 36,900 kN, and R_d and R_o were 2.0 and 1.5, respectively, resulting in a base shear of 995 kN. The ESFP distributes the base shear over the height of the building as a concentrated force at each storey level (F_x) according to Eq. (2):

$$F_x = \frac{(V-F_t)W_x h_x}{\sum W_i h_i} \tag{2}$$

where W_x is the seismic weight of floor *x* and h_x is the height at floor *x*. Finally, the ESFP requires a portion of the base shear (F_t) to be concentrated at the top of a building when the fundamental period is greater than 0.7 s. The remainder, $V - F_t$ is to be distributed along the height of the building including the top level where F_t is concentrated. F_t is equal to $0.07T_aV$ but cannot exceed $0.25V$. For this prototype building F_t is equal to 110 kN (0.07 × 1.6 s × 995 kN). The design of the prototype structure also included consideration for torsional effects. Because the building was square and symmetric in plan, torsional effects would be minimal, however, accidental torsion was still considered in the building design. This approach consisted of applying the lateral earthquake force at each storey level at an eccentricity equal to 10% of the building width.

Brace and Connection Design

The diagonal members in the braced frame were designed for the maximum tension and compression forces based on the structural analysis. Different brace and connection sizes were used every two storeys (i.e., 4 different connection designs over the building height). While the approach to designing the brace and connections is the same for each level, the first floor brace and connection are discussed here as they will be the subject of the experimental program described in this study, which had a factored design load of 245 kN. For all aspects of the member design, service condition, and treatment factors were assumed to be 1.0.

The brace size was determined based on the desired bolt slenderness ratio of 12, which is higher than the recommendation of 10 in Eurocode 5 but was selected in an attempt to maximize the ductility of the connections [8]. The connection was assumed to have two slotted-in steel plates and a bolt diameter of 9.53 mm (3/8”). In a connection with two slotted-in steel plates, the bolt slenderness ratio is defined as the distance between the slotted-in steel plates divided by the bolt diameter. Based on a slenderness ratio of 12, the minimum brace dimension was calculated as 12 × 9.53 × 2 + 20 = 250 mm, where the additional 20 mm accounts for the thickness of two 10 mm thick slotted-in steel plates. The closest standard glulam size to 250 mm is 265 mm, which was chosen as the brace width in one direction. A preliminary size for the other brace dimension was chosen based on the compression and tension resistance of the brace, which was 190 × 265 mm, governed by brace resistance in compression.

A preliminary geometry of the glulam brace was required to initiate the design of the brace end connections, which were designed to fail in a ductile manner. The brace connections were bolted with slotted-in steel plates, which is an appealing connection type because the steel plates are concealed within the timber in case of fire and steel bolts, or tight-fit pins are readily available in a wide range of sizes and grades. The connection design considered brittle and ductile failure mechanisms, illustrated in Figure 4, which include: (1) net tension, (2) row shear, (3) group tear-out, and fastener yielding.

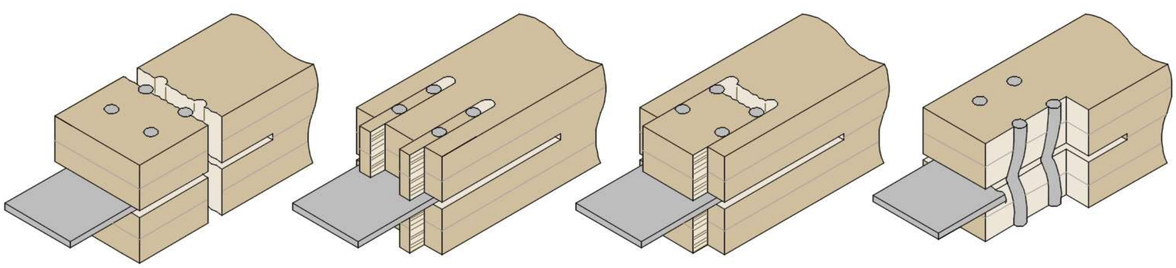

(a) (b) (c) (d)

Figure 3. Connection failure mechanisms (a) net tension; (b) row shear; (c) group tear-out, (d) dowel yielding.

To ensure the connection would exhibit ductile behaviour in the event of an earthquake dowel yielding (illustrated in Figure 3(d)) was the intended mode of failure. In addition to dowel yielding, it is recognized that connections that use dowels with larger slenderness exhibit more ductile behaviour and can sustain large plastic deformations [5]. Based on a dowel diameter of 9.53 mm (3/8”), the number of dowels required to achieve a resistance of at least 245 kN was determined using the provisions in CSA O86-19. The factored lateral yielding resistance (N_r) of a group of fasteners in a connection is computed using Eq. (3):

$$N_r = \emptyset_y n_u n_s n_F \tag{3}$$

where φ_y is the resistance factor for yielding factors, taken as 0.8, n_u is the unit lateral yielding resistance, n_s is the number of shear planes in the connection and n_F is the number of fasteners in the connection. The connections in the prototype structure were designed with 2 slotted-in steel plates, which results in 4 shear planes. The unit lateral yielding resistance, n_u, is taken as the smallest unit lateral yielding resistance for various dowel yielding modes. For this connection the smallest value of n_u was associated with the yielding mode d in CSA O86-19, which is determined using Eq. (4):

$$n_u = f_1 d_F^2 \left(\sqrt{\frac{2}{3} \frac{f_2}{(f_1+f_2)} \frac{f_y}{f_1}} \right) \tag{4}$$

where f_1 and f_2 are the embedment strengths of members 1 (side) and 2 (main), d_F is the diameter of the fastener, t_1 and t_2 are the member thickness or dowel bearing length of members 1 and 2, and f_y is the yield strength of the fastener in bending. The embedment strengths of members 1 and 2 were 19.9 MPa and 1350 MPa for the glulam and the steel plates, and member thicknesses were 61.5 mm and 10.0 mm, which were equal to the dowel bearing length. The bolts were assumed to be grade ASTM A307, with a yield strength (f_y) of 310 MPa. The slotted-in steel plates were assumed to be grade 350W steel with a yield strength (f_y) of 350 MPa and an ultimate tensile stress (f_u) of 450 MPa. This resulted in a unit lateral yielding resistance of 267 kN, and thus, a total of 16 steel bolts were required to ensure the connection had a yielding resistance greater than the design load (T_f = 245 kN).

In addition to considering yielding of the fasteners, the connection design also considered the brittle failure modes, illustrated in Figure 3. The connection was designed with the goal of having a ratio of brittle resistance over ductile resistance of 2.0 or greater in an attempt to ensure that ductile behaviour is achieved. The value of such over-strength factor has not been investigated in the literature or reported in the timber design standard [1]. A factor of 2.0 was considered adequately conservative for this purpose. The parallel-to-grain row shear resistance (PR_{rT}), was determined using Eq. (5):

$$PR_{rT} = \sum(PR_{ri}) \tag{5}$$

where PR_{ri} is the sum of the wood members resisting the load, which is determined using Eq. (6):

$$PR_{ri} = \emptyset_w PR_{ij\,min} n_R \tag{6}$$

where φ_w is the resistance factor for brittle failures and n_R is the number of fastener rows, through summing the factored row shear resistance of the wood members resisting the load, PR_{ri}. The resistance factor for brittle failures is 0.7 and the number of fastener rows for this connection is 4. Finally, the row shear resistance of any row of the connection (PR_{ij}) is determined using Eq. (7):

$$PR_{ij} = 1.2 f_v (K_D K_{Sv} K_T) K_{ls} t n_c a_{cri} \tag{7}$$

where f_v is the specified strength in shear for member i, k_{ls} is the factor for member loaded surface, t is the member thickness, n_C is the number of fasteners in row j of member i, a_{cri} is the minimum of a_L and S_R for row j of member i, K_D is the load duration factor, K_T is the treatment factor, and K_{Sv} is the service condition factor for longitudinal shear. a_L is the loaded end distance and S_R is the spacing of fasteners in a row. For the connections considered in this study, the wood member has a specified strength in shear of 2.5 MPa, the side and internal members have a factor for member loaded surface of 0.65 and 1.0, respectively, and the number of fasteners in a row is 4 and a load duration factor of 1.15 was used because earthquake loads are considered short-term loads. The minimum allowable spacing between fasteners in a row (S_R) according to CSA O86 is equal to four bolt diameters ($4d_f$), resulting in a spacing of 40 mm and a row shear capacity of 353 kN, which translated into 1.3 times the capacity associated with yielding (1.3 ratio of brittle/ductile failure).

This design does not result in a ratio of brittle to ductile failure of 2.0 or greater, which was one of the design objectives of this study. To achieve a brittle/ductile capacity ratio of 2.0, the fastener spacing was increased to 90 mm ($9d_f$), which resulted in a capacity of 545 kN governed by group tear-out (brittle/ductile = 2.0). However, to better understand the influence of fastener spacing on the connection behaviour, a second connection with a fastener spacing of 45 mm ($4.5d_f$) was also designed and tested as part of the experimental program to investigate the influence of fastener spacing on the connection behaviour.

The total factored parallel-to-grain group tear-out resistance of a connection, PG_{rT}, was calculated using Eq. (8):

$$PG_{rT} = \sum(PG_{ri}) \tag{8}$$

where PG_{ri} is the factored group tear-out resistance of fasteners in a wood member i with n_R rows and is calculated using Eq. (9):

$$PG_{ri} = \emptyset_w \left[\frac{PR_{i1}+PR_{inR}}{2} + f_t(K_D K_{St} K_T)A_{PGi}\right] \tag{9}$$

where f_t is the specified strength in tension and A_{PGi} is the critical perpendicular net area between rows 1 and n_R of member i. The glulam has a specified strength in tension of 17 MPa and a critical net area between the first and last rows of fasteners of 6730 mm^2. The shear resistance along row 1 of fasteners bounding the fastener group (PR_{i1}) and along row n_R of fasteners bounding the fastener group (PR_{iNR}) were calculated using Eq. (10) and Eq (11), respectively:

$$PR_{i1} = 1.2 f_v(K_D K_{Sv} K_T)K_{ls} t n_c a_{cr\ 1} \tag{10}$$

$$PR_{inR} = 1.2 f_v(K_D K_{Sv} K_T)K_{ls} t n_c a_{cr\ nR} \tag{11}$$

This resulted in group tear-out capacities of 545 kN and 457 kN for the connections with 90 mm and 45 mm spacing, respectively. The initial brace size of 190 x 265 mm required the row spacing to be the minimum allowable ($3d_F$) which caused the group tear-out capacity to be 343 kN instead of 545 kN which yielded a ratio of brittle over ductile resistance of 1.3 which did not meet the goal of 2.0 or greater. Therefore, the member size was increased to 265 x 266 mm in order to increase the row spacing to 50 mm and result in a sufficient group tear-out resistance. The connection with 90 mm bolt spacing has a ratio of brittle resistance to ductile resistance of 2.0 (governed by group tear-out), while the connection with 45 mm bolt spacing has a ratio of brittle resistance to ductile resistance of 1.3 (governed by row shear). Lastly, based on the brace size of 265×266 mm, the net tension resistance of the member ($T_{Nr\ T}$) was calculated using Eq. (12):

$$T_{Nr\ T} = \sum T_{Nr\ i} \tag{12}$$

where $T_{Nr\ i}$ is the total factored net tension resistance of member i at a group of fasteners, calculated as the lesser of the net tensile resistance or the gross tensile resistance in Eq. (13) and Eq. (14), respectively:

$$T_r = \emptyset F_{tn} A_n \tag{13}$$

$$T_r = \emptyset F_{tg} A_g \tag{14}$$

where the φ is the tensile resistance factor of 0.9, F_{tn} is the specified strength in tension parallel to grain at the net section, F_{tg} is the specified strength in tension parallel to grain at the gross section, A_n is the net area of the cross-section, and A_g is the gross area of the cross-section. The specified strengths in tension parallel to grain at the net section and gross section are 17 MPa and 12.7 MPa, respectively, and the net and gross areas of the cross-section are 51876 mm^2 and 65190 mm^2, respectively, which results in a net tension capacity of 913 kN for the brace member. Figure 4 illustrates the design for a representative first-storey bay of the prototype structure, including the brace end connections.

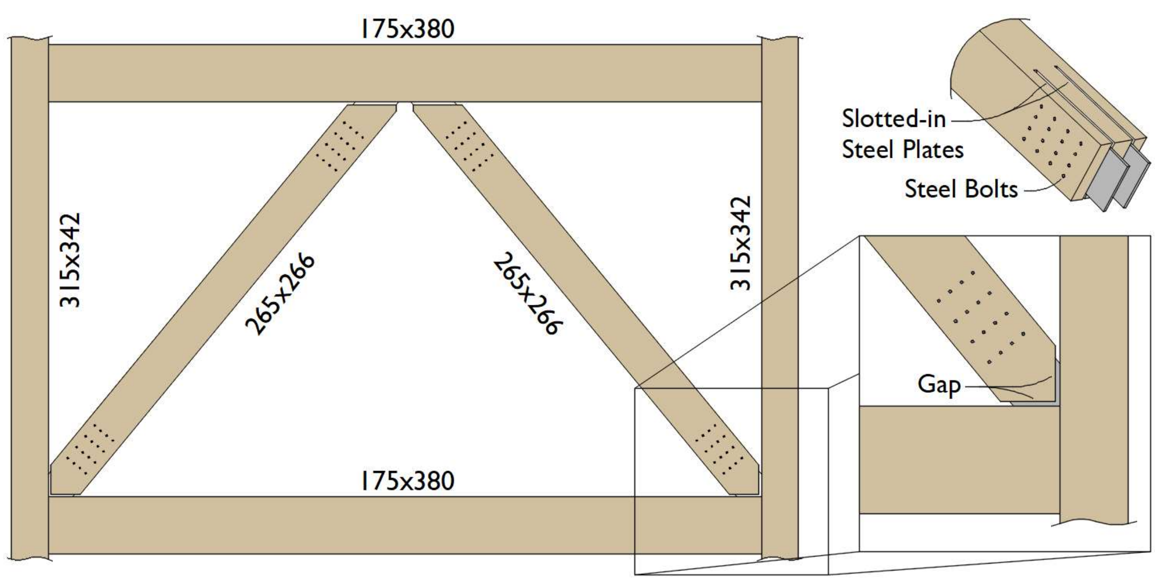

Figure 4. Representative braced timber frame bay and connection detail.

Table 3. Connection Design Summary.

	Connection C-45 (45 mm Bolt Spacing)	**Connection C-90 (90 mm Bolt Spacing)**
Factored Load (kN)	245	245
Yielding Resistance (kN)	267	267
Row Shear Resistance (kN)	353	706
Group Tear-Out Resistance (kN)	457	545
Net Tension Resistance (kN)	913	913
Ratio of Ductile to Brittle Resistance	1.3	2.0
Slenderness Ratio	13	13

EXPERIMENTAL PROGRAM

The previous section described the procedure used to design and detail a moderately ductile timber braced frame and representative connection according to the provisions of the CSA O86-19. However, there is a lack of understanding on whether such connections will be capable of achieve the desired connection-level ductility. To better understand the ductility of the proposed design connection, two configurations were tested at full-scale.

Figure 5 shows the two connection configurations tested in this study. The specimens were 1.375 m long and included two connections tested under cyclic loading. The cyclic loading was in tension only due to out of plane displacement of the test setup under compression. This specimen configuration permitted evaluation of the deformation and ductility each individual connection in a full-scale brace might experience, including evaluating the potential for disproportionate maximum deformation levels amongst two identical connections that have been observed in past research [9-10]. The two connection configurations had identical geometry except for the fastener spacing, which was either 90 mm or 45 mm. These connections are hereafter referred to as connections C-45 and C-90, respectively, as illustrated in Figure 5.

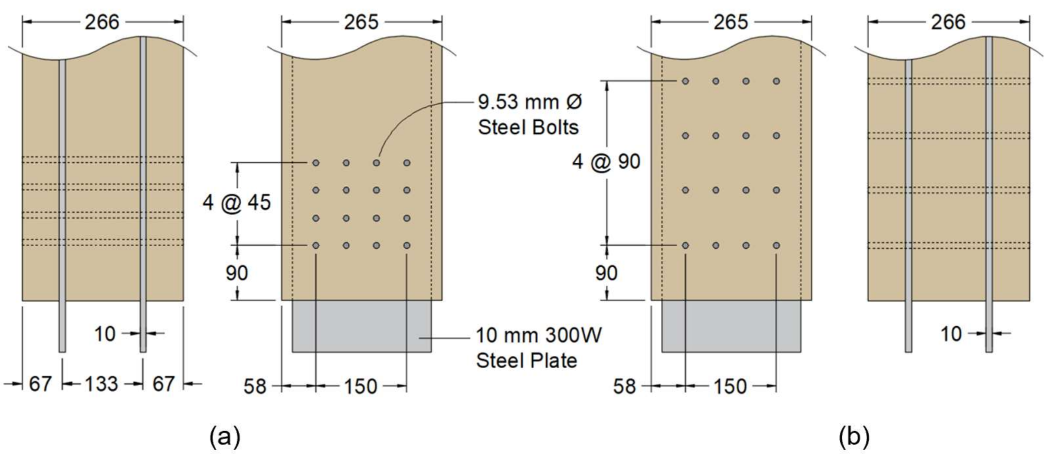

Figure 5. Connection configurations (units in mm): (a) C-45; (b) C-90.

Material Properties

The connections were fabricated from grade 24f-E spruce-pine glulam supplied by Nordic Structures in Quebec, Canada. According to the manufacturer, the glulam has a density of 560 kg/m^3, a tension strength parallel to grain at gross section of 12.7 MPa, a tension strength parallel to grain at net section of 17 MPa, and a compression strength parallel to grain of 25.2 MPa, and a modulus of elasticity of 13.1 GPa [7]. The steel bolts used in the connection tests were 9.53 mm (9/16") diameter and were grade ASTM A307. The properties of the steel bolts were determined by conducting tension tests on three coupons according to the ASTM E8/E8M test method [11]. Results demonstrated that the bolts have an average yield stress of 420 MPa with a standard deviation (SD) of 8.0 MPa and an ultimate stress of 478 MPa (SD = 6.5 MPa).

Loading Protocol and Experimental Test Setup

Figure 6 shows the experimental test setup for the connection tests described in this study. The connections were tested under cyclic loading using an actuator with a 250 mm stroke and a capacity of 1350 kN in tension. The test setup was the same for the monotonic test as well as the two cyclic tests. The top slotted-in steel plates were welded to a plate that was connected to the actuator using 4 – 38.1 mm (1-1/2") steel bolts. The bottom slotted-in steel plates were welded to a plate that was connected to a large steel assembly using 20 – 19.1 mm (3/4") bolts. The large steel assembly was fixed to the lab strong floor using 8 –

31.8 mm (1-1/4") grade B7 steel rods. Lateral out-of-plane support was provided to prevent the assembly from buckling in the out-of-plane direction during cyclic loading. The cyclic loading was applied in tension only due to some out-of-plane buckling even with the lateral support braces. To measure the displacement response of the connections, four string potentiometers were used, including two to measure the displacement of the top and bottom connections, respectively. Linear potentiometers were also used to measure any displacement between the steel assembly and the strong floor and any opening of the slots in the timber for the steel plates.

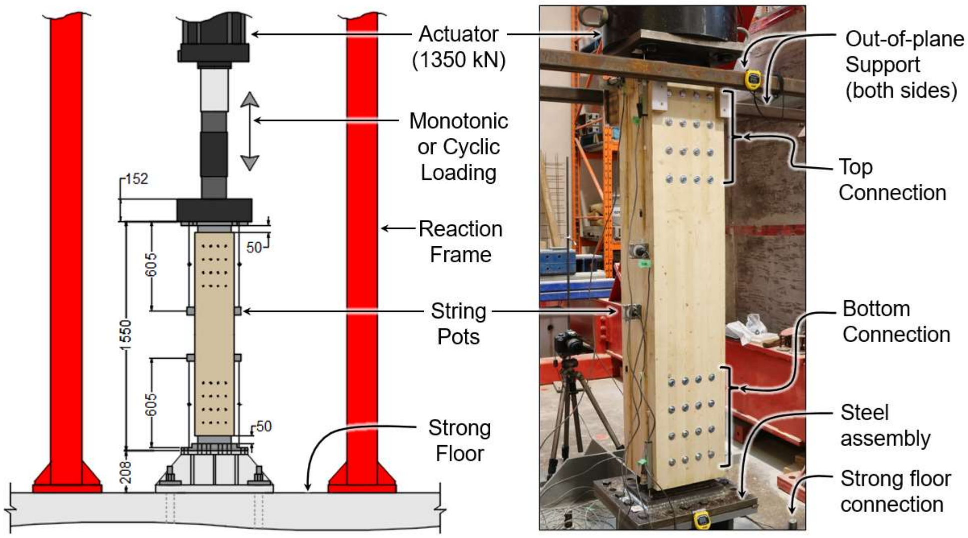

Figure 6. Experimental test setup.

Overall, three full-scale connection tests are described in this paper. Connection C-90 (Figure 5(a)) was tested under both monotonic and cyclic loading (referred to as C-90-M and C-90-C, respectively). Connection C-45 (Figure 5(b)) was tested under cyclic load to directly compare the implications of a smaller fastener spacing on seismic behaviour, including ductility and energy dissipation capacity (referred to as C-45-C). The loading protocol used for both the monotonic and cyclic tests was based on the European Test Standard EN12512 – *Cyclic Testing of Joints made with Mechanical Fasteners* [12]. The monotonic tests were conducted at a displacement-controlled rate of 2 mm/min. The yield displacement (Δ_y) from the monotonic test (C-90-M) was used to define the cyclic loading protocol. Figure 7 shows the loading protocol for the tensile cyclic connection tests. Based on the EN12512 cyclic loading protocol, displacement increments of 0.2, 0.4, 0.6, 0.8, 1.0, 1.5, and 2.0 times the yield displacement were applied, followed by increments of Δ_y up to failure.

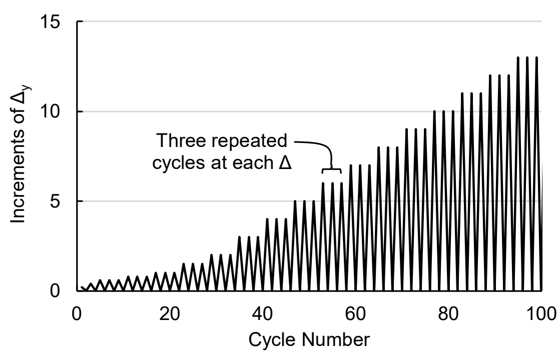

Figure 7. Cyclic loading protocol [12].

EXPERIMENTAL RESULTS AND DISCUSSION

Table 4 summarizes the important structural response parameters from the experimental connection tests, including the yield load and displacement (P_y, Δ_y), peak load displacement (P_{peak}, Δ_{peak}), and ultimate load and displacement (P_u, Δ_u) for both the top and bottom connections in each specimen. The connection ductility (μ_c) was determined as the ratio of the ultimate and yield displacement of the connection ($\mu_c = \Delta_u / \Delta_y$). Numerous methods exist in the literature to evaluate the yield displacement in timber connections [13-14]. In this study, the Yasumura and Kawai (Y&K) Method was used to determine the yield load and displacement for each connection, which has been shown to produce consistent results amongst a range of connection types

[12]. A backbone curve of the cyclic response was used to determine the parameters in Table 4. The ultimate load and displacement were taken as the point on the force-displacement graph where the load dropped by 20% from the peak load.

Table 4. Connection Force-Displacement Response Parameters.

	C-90-M		C-90-C		C-45-C	
Parameter	**Top**	**Bottom**	**Top**	**Bottom**	**Top**	**Bottom**
P_y (kN)	625	625	502	503	540	447
Δ_y (mm)	3.93	3.00	4.21	4.28	5.43	5.00
P_{peak} (kN)	1004		777		635	
Δ_{peak} (mm)	20.0	15.2	18.2	17.6	7.91	7.28
P_u (kN)	803		621		508	
Δ_u (mm)	20.4	15.6	22.7	24.3	26.17	16.5
Ductility	5.19	5.21	5.39	5.67	4.82	3.30

Monotonic Test (C-90-M)

Figure 8(a) shows the force-displacement response of the top and bottom connection for the monotonic test with 90 mm bolt spacing (C-90-M). It is noted that the connection reached the maximum capacity of the test system and did not fail, however, both top and bottom connections exhibited significant plastic deformation and splitting of the specimen, shown in Figure 8(b), prior to unloading. The force-deformation relationship shows an initial slip, in which the gap between the bolts and the steel plates closed, which is followed by an elastic response up to yield. The top and bottom connections had initial stiffnesses of 265 kN/mm and 380 kN/mm, respectively, which were measured between 40 % and 80 % of the yield load. Both top and bottom connections yielded at identical loads of 625 kN. After yielding, both connections exhibit hardening behaviour due to the embedment strength of the wood interacting with the bolts as they continue to yield. The onset of splitting in the top and bottom connections occurs at displacements of 9.0 and 4.0 mm, respectively. Under increasing displacement, the degree of splitting increases throughout the test duration. The maximum load that could be applied given the test setup was reached and therefore neither of the connections failed during the monotonic test. Once the maximum load was reached the member was cycled in tension from the maximum capacity to zero displacement three times.

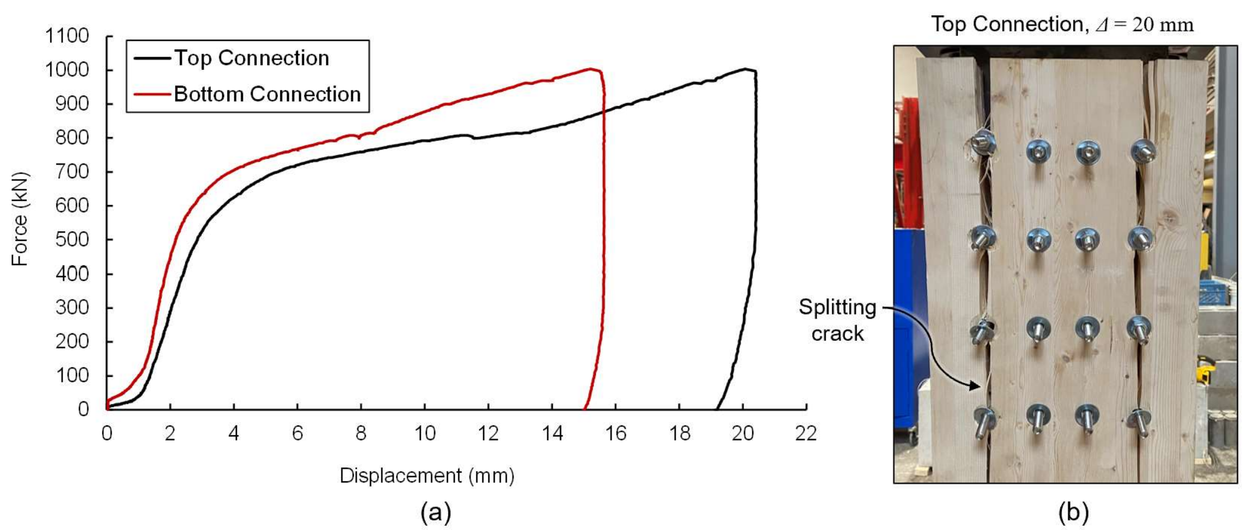

Figure 8. Force-deformation behaviour: (a) C-90-M, (b) Top Connection at End of Test.

Cyclic Test Results (C1 and C2)

Figure 9(a) shows the hysteretic force-displacement response for connection C-90-C, which has a similar behaviour to connection C-90-M (based on the backbone curves). The behaviour of the connection includes an initial slip response followed by an elastic response up to nearly identical yield loads of 502 kN and 503 kN for top and bottom connections, respectively. The initial stiffness of the top and bottom connections were 295 and 325 kN/mm, respectively, and were within 10 % of one another. The post-yield stiffness of connection C-90-C is smaller compared with the monotonic result, which may be attributed to stiffness and strength degradation under cyclic loading. Nonetheless, both top and bottom connections exhibit significant plastic deformation capacities and had ductility ratios of 5.21 and 5.39, respectively, resulting in overall ductility of 10.6.

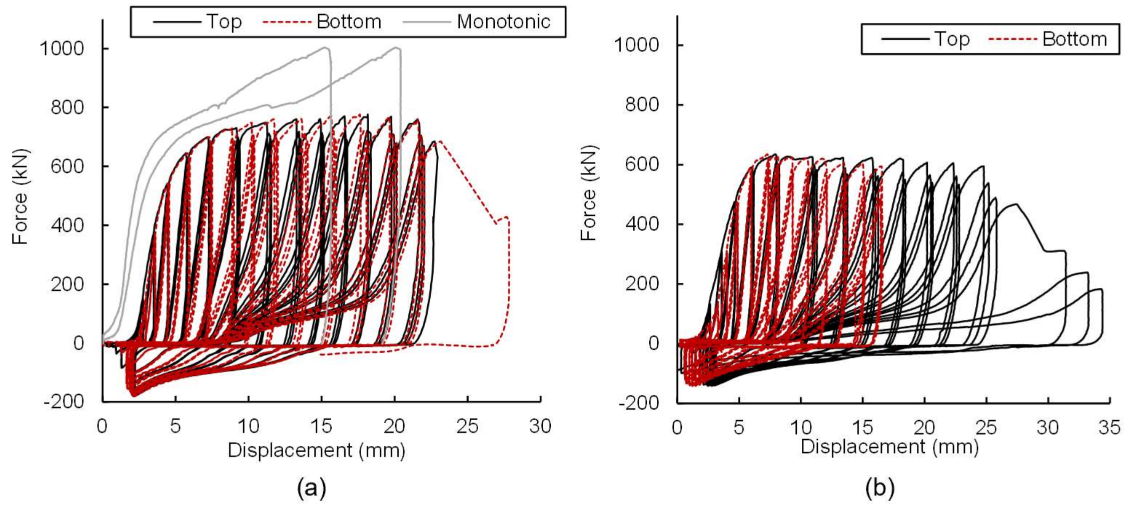

Figure 9. Force-deformation behaviour: (a) C-90-C, (b) C-45-C.

Figure 9(b) shows the hysteretic force-displacement response for specimen C-45-C. The results once again show high initial stiffness of the connections, which were 170 and 340 kN/mm for top and bottom connections, respectively. Based on a comparison to the stiffness observed in C-90-C the fastener spacing had a negligible influence on the initial stiffness of the connection. The yield load of the top and bottom connection of 540 and 447 kN are also comparable to specimen C-90-C. The primary differences amongst the specimens are observed in the post-yield response, which shows lower post-yield stiffness and high strength degradation under cyclic loading for connection C-45-C. This is attributed to the fastener spacing, as specimen C-45-C had close to the minimum allowable bolt spacing from CSA O86-19 of $4d_f$. The smaller bolt spacing resulted in splitting in the perpendicular to grain direction to occur sooner, causing higher strength degradation under cyclic loading. The negative post-yield stiffness also meant that both connections did not yield by the same amount, as the top and bottom connections had ductility ratios of 4.82 and 3.30, respectively, resulting in an overall member ductility of 8.12, assuming both connections yield, which is lower than the overall ductility of 10.6 that was achieved in C-90-C.

CONCLUSIONS AND FUTURE WORK

This paper describes the design process for an 8-storey mass timber braced frame building and the test results obtained from a full-scale connection from the building investigated under monotonic and cyclic loads. The following conclusions were drawn:

1. Glulam brace connections with multiple slotted-in steel plates can achieve the strength requirements for mid-rise mass timber braced frame structure design in regions of moderate seismicity.
2. Experimentally tested bolted glulam brace connections with slotted-in steel plates exhibited ductility ratios of larger than 10, including significant plastic deformations in both brace connections when detailing a dowel slenderness ratio of 12.0 and a ratio of brittle/ductile failure modes of 2.0.
3. Increasing the bolt spacing from the minimum spacing recommended by CSA O86 of $4d_f$ to $10d_f$ delayed the onset of splitting in the connection, reduced strength degradation, and resulted in a 30 % increase in the brace ductility from 8.12 to 10.6.

The results discussed in this paper are part of a larger study on the performance of full-scale bolted glulam brace connections under axial load. The goal of this project is to provide recommendations and practical detailing guidance on how to design ductile connections to ensure the system-level ductility requirements in NBCC can be achieved. This work includes a series of large-scale connection tests with different configurations, including member size, length and diameter of the fastener, fastener spacing, and the use of self-tapping screws as perpendicular-to-grain reinforcement.

ACKNOWLEDGMENTS

The Authors gratefully acknowledge the financial support provided by the Natural Sciences and Engineering Research Council of Canada. The Authors would also like to thank Justin Bennett, Jared Mason and Jodie Goodwin for their support in executing the large-scale experiments.

REFERENCES

[1] CSA (2019). “Engineering Design in Wood.” *Canadian Standards Association CSA O86-19.*

[2] NRC (2015). “National Building Code of Canada.” *National Research Council of Canada.*

[3] Masroor Mohammad, Doudak Ghasan, and Casagrande Daniele, “Design of Multipanel CLT Shear Walls with Bidirectional Mechanical Anchors Following Capacity-Based Design Principle,” *Journal of Performance of Constructed Facilities*, vol. 36, no. 1, p. 04021113, Feb. 2022, doi: 10.1061/(ASCE)CF.1943-5509.0001693.

[4] Casagrande Daniele, Doudak Ghasan, Mauro Luigi, and Polastri Andrea, “Analytical Approach to Establishing the Elastic Behavior of Multipanel CLT Shear Walls Subjected to Lateral Loads,” *Journal of Structural Engineering*, vol. 144, no. 2, p. 04017193, Feb. 2018, doi: 10.1061/(ASCE)ST.1943-541X.0001948.

[5] FP Innovations (2022). “Modelling Guide for Timber Structures – First Edition”. *FP Innovations,* Special Publication SP-544.

[6] CWC. 2017. *Wood Design Manual*. Ottawa: Canadian Wood Council.

[7] Nordic Structures. (2022). Mass Timber Construction: Nordic LAM+ Technical Guide, Nordic Structures, Montreal.

[8] “Eurocode 5: Design of timber structures - Part 1-1: General - Common rules and rules for buildings.” European Standard, 1995.

[9] Chen Zhiyong and Popovski Marjan, “Seismic Response of Braced Heavy Timber Frames with Riveted Connections,” *Journal of Performance of Constructed Facilities*, vol. 35, no. 5, p. 04021051, Oct. 2021, doi: 10.1061/(ASCE)CF.1943-5509.0001618.

[10] Z. Chen and M. Popovski, “Connection and System Ductility Relationship for Braced Timber Frames,” *Journal of Structural Engineering*, vol. 146, p. 04020257, Sep. 2020, doi: 10.1061/(ASCE)ST.1943-541X.0002839.

[11] “ASTM E8/E8M - 22 Standard Test Methods for Tension Testing of Metallic Materials.” ASTM International, Jul. 19, 2022.

[12] “EN12512 Timber structures - Test methods - Cyclic testing of joints made with mechanical fasteners.” European Committee for Standardization, Nov. 2001.

[13] W. Munoz, M. Mohammad, A. Salenikovich, and P. Quenneville, “Determination of Yield Point and Ductility of Timber Assemblies: In Search for a Harmonised Approach”.

[14] Yasumura, M., and N. Kawai. 1998. Estimating seismic performance of wood-framed structures. *Proceedings of 1998 I.W.E.C.* Switzerland. Vol.2. pp. 564-571.